

# ERT method in the study of chemical pollution of the hydrogeological environment – numerical analysis of 2D and 3D models

Grzegorz Bania\*

AGH University of Science and Technology, Faculty of Geology, Geophysics and Environment Protection, Kraków, Poland

**Abstract.** Electrical resistivity tomography (ERT) method is often used to solve problems related to chemical pollution of the hydrogeological environment. The source of such contamination can be, e.g. industrial heaps, tailings ponds and municipal landfills. The contaminants spreading often takes the form of a (3D) pollution tongue. In this case, the standard interpretation of 2D ERT surveys may be difficult. Numerical modeling was carried out in order to show the specificity of pollutants propagation. Both 2D and 3D models were analysed. Those refer to the real geological situation – vicinity of Nowa Huta (Krakow, Poland) – where heaps and tailings ponds of the metallurgical plant are present. An appropriate geoelectrical model referring to the above situation was prepared. It was assumed that highly mineralized waters in the form of a contamination tongue are spreading within the aquifer. Resulting interpreted resistivity distributions for 2D and 3D variant of ERT method were analysed. It has been shown that the method is promising in terms of the ability to detect and assess the nature of the transitional zone between clean and contaminated waters. Additionally, it has been shown that 3D modeling can be a useful, complementary element in interpreting the results of DC-resistivity methods.

**Keywords:** DC-resistivity method, ERT, electrical resistivity tomography, modeling, groundwater pollution

## 1 Introduction

The DC-resistivity method, including the electrical resistivity tomography (ERT) method, is used particularly often in studies related to groundwater contamination caused by the impact of different types of landfills [e.g. 1-9]. The aim of the study was to show the possibility of using the ERT method for solving problems related to groundwater pollution of wastes from metallurgical origin (and not only) through numerical modeling. Modeling is an additional tool that allows to check how a given situation, e.g. spatial hydrogeological structure described by physical parameters (geophysical model), will be reflected in simulated measurements results and inversion. Moreover it allows to analyse various scenarios and to

---

\* Corresponding author: [bania@agh.edu.pl](mailto:bania@agh.edu.pl)

consider potential limitations of the DC-resistivity method in order to select the appropriate measurement methodology.

The work concerns two-dimensional (2D) and three-dimensional (3D) models of the hydrogeological center in relation to the real terrain situation – vicinity of Nowa Huta (Krakow, Poland) [9-10]. These models simulate a hypothetical pollution tongue/cloud that penetrate into the groundwater. The source of contamination may be, e.g. a heap or tailings pond of the metallurgical plant. This pollution cloud indicates a targeted displacement of low resistivity contaminants within the assumed aquifer. During the construction of the models, the results and conclusions from the research concerning groundwater pollution in vicinity of the Zelazny Most tailings pond (derived from the copper ore enrichment in KGHM) [4, 11] were taken into account. In that case, the use of geoelectrical methods proved to be very effective.

## 2 Creation of geoelectrical models

Referring to the real geological situation from the vicinity of Nowa Huta (Krakow, Poland), a typical lithological profile was created (Fig. 1). There is 3 m of overburden (soil, sandy loam). Deeper, there are layers of sand and sandy gravel which constitute aquifer with a thickness of 7 m. The deepest layer (10 m under the surface) is made of clay which is impermeable and prevents penetration of contaminants into the deeper parts of the center. On the basis of the lithological profile, two resistivity models were created - A, which assumes unpolluted water within the aquifer and B, which simulates contaminated medium (Fig. 1). Due to the similar resistivity characteristics of sands and gravels, they are treated as one layer. For simplification, the appropriate rock model was used [12]. In this model, one component is the rock skeleton (spherical, homogeneous grains) and the second one, mineralized water that fills its pores.

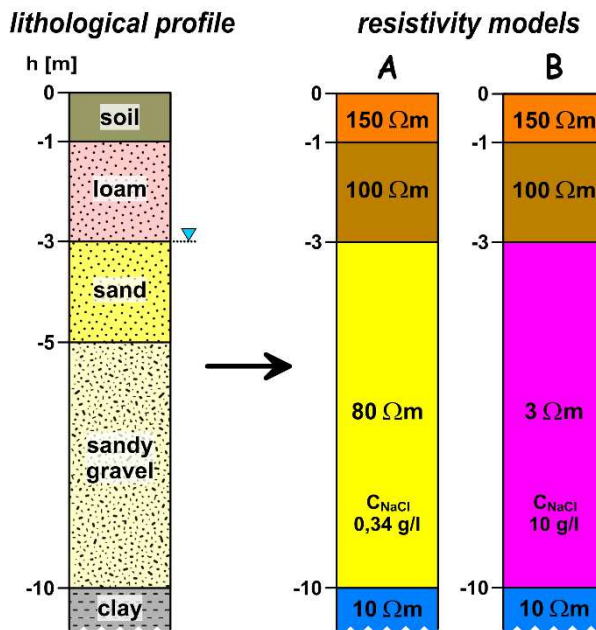


**Fig. 1.** Typical lithological profile from the vicinity of Nowa Huta and corresponding resistivity models.

In the model (Fig. 1) it was assumed that the aquifer had a temperature of 10 °C and water filling the pores was saturated with NaCl with a concentration of 0.34 g/l. Based on the dependence of resistivity to the mineralization of the NaCl solution [13], the water resistivity was determined to be 22.7 Ωm. Additionally, it was assumed that the sand grains (quartz) are practically non-conductive and taking the porosity coefficient  $K = 0.37$  the resultant resistivity of the aquifer was calculated – 80 Ωm. In addition, in the considered geoelectrical models, overburden resistivities of 150 and 100 Ωm were assumed. The resistivity of the clay layer was assumed to be 10 Ωm. The chosen value is characteristic for clays that can be found in the vicinity of Nowa Huta, i.e. approx. 10-20 Ωm [10].

For the needs of 2D and 3D modeling it was assumed that the layers of the geoelectrical models (Fig. 1) are homogeneous and isotropic and a layer with a resistivity of 80 Ωm (model A) will be the background for the pollution cloud spreading within it. It was assumed that the mineralization of contaminated waters is 10 g/l. The calculated resistivity of contaminated water is 0.87 Ωm. The resultant resistivity value for the contaminated layer was determined - 3 Ωm (model B).

## 2.1 2D models

2D models were created in the Res2Dmod software [14]. Two situations were analysed - M1 and M2 (Fig. 2) which simulate two different types of the front of moving pollution tongue. In both models 2 m electrode spacing and two mesh blocks between adjacent electrodes were used. Vertically, up to a depth of 10 m, the mesh blocks have a fixed height of 0.5 m, and from 10 m in depth their height is gradually increasing. The visibility of the models and inversion results was limited to about 15 m in depth and it was assumed that the last layer continues deep into infinity. It should be emphasized that the 2D model is being considered, i.e. it does not change its properties in the direction perpendicular to the measurement line. In fact, the medium is heterogeneous and anisotropic and as a result of inversion this leads to the interpretation of artifacts related to the 3D effect (side effect) [e.g. 15].

The M1 model (Fig. 2) simulates a situation in which the front of pollution cloud is fuzzy, i.e. changes in the resistivity proceed in a gradient manner creating a transitional zone between the contaminated (3 Ωm) and clean (80 Ωm) waters. Such situation may be suitable for a relatively slow moving pollution tongue or in the case where the tongue will stop moving and contaminated waters will gradually mix with the sweet ones. Model M2 (Fig. 2) considers the situation of a rapid movement of pollution cloud which, in the resistivity model can be presented with sharp boundary between the resistivity layers of 3 and 80 Ωm. In addition, for both models, the border between contaminated and clean centers is not vertical but tilted.

Simulated apparent resistivity pseudosections were calculated for dipole-dipole array with current and potential dipoles  $a = 1, 2, 3, 4, 5, 6 \Delta x$  and distances between these dipoles, respectively  $n = 1, 2, 3, 4, 5, 6 a$ . Inversion of the data was carried out in the Res2Dinv software [16]. The inversion process based on the L1-norm (robust) inversion method have been applied. The obtained inverse model resistivity sections have been compiled under the models in Figure 2. For better comparison of modeled situations with inversion results, the real horizontal boundaries between the model layers were marked in the sections. In addition, the external borders of the transitional zone for the M1 model and the border between contaminated and clean centers in the case of the M2 model were marked.

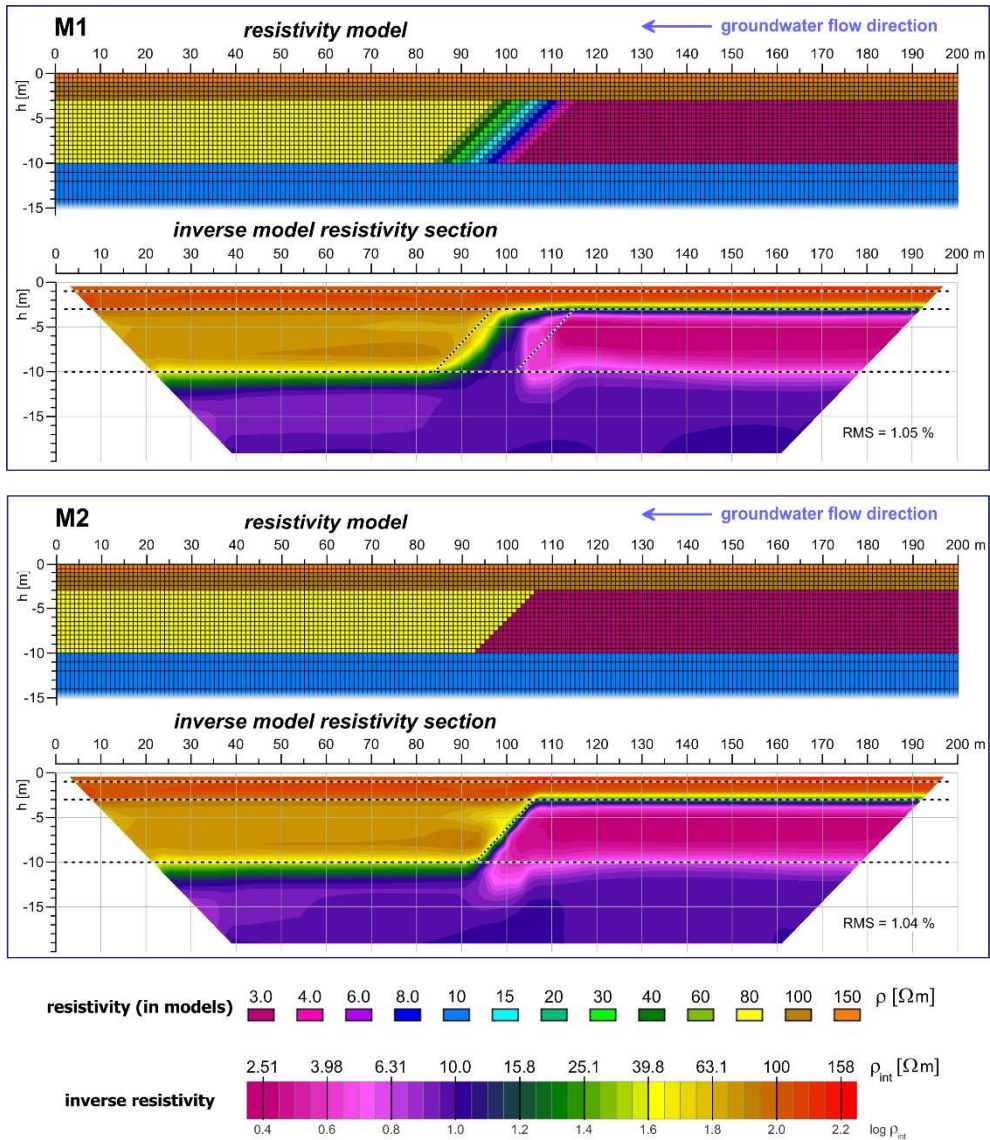


**Fig. 2.** 2D resistivity models showing two types of the front of pollution cloud together with corresponding inversion results.

## 2.2 3D model

The 3D model of the pollution tongue was created in the Res3Dmodx64 software [17]. Creating this model (Fig. 3a), subsequent layers / depth levels were reflected exactly as in the assumed geoelectrical model (Fig. 1). Similarly to the 2D models (Fig. 2), the heights of individual blocks to a depth of 10 m are 0.5 m which gives 20 depth levels. Below this depth there are additional layers with gradually increasing height of blocks, which is partially visible in the section in Figure 3c. Horizontal grid dimensions (x, y) in all model depth levels are 100 x 100 (Fig. 3b). Two nodes between adjacent electrodes (with 2 m spacing) in the x and y directions were applied. In total, this gives the number of electrodes 51 x 51 = 2601. Note that using such a large number of electrodes in field measurements would be very

troublesome. For this reason, the proposed 3D model (Fig. 3) should be considered only hypothetically. Figure 3b shows the selected depth level of the model - from -5.0 to -5.5 m. It can be noticed that the shape of the tongue is not symmetrical. This is to refer to real conditions and causes an additional "difficulty" for the inversion process, which task is to recreate the original model. The hypothetical source of pollution is placed outside the model, over 30-50 m on the x axis. It was assumed that the dominant direction of groundwater flow is consistent with the A-A' section line marked in Figure 3. The front of the pollution cloud, well visible on the section A-A' (Fig. 3c), was designed in a similar way to the 2D M2 model (Fig. 2). In the direction corresponding to the x axis (Fig. 3b), there is also the spread of the contaminated waters. It is consistent with the visible gradient zone proposed in the 2D M1 model (Fig. 2).

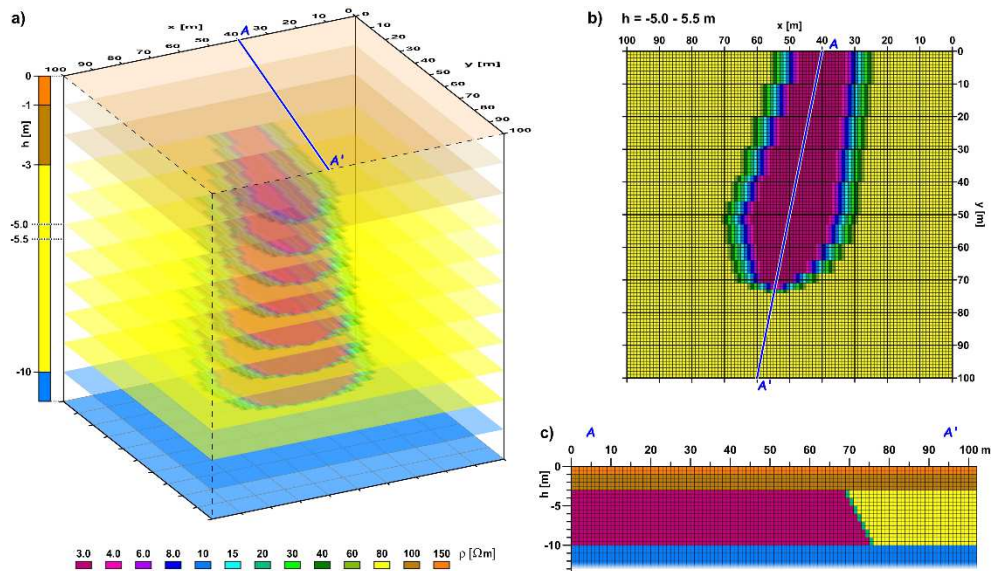


**Fig. 3.** 3D resistivity model of a pollution tongue: a) simplified, general view; b) example of model's depth level (bird's eye view); c) A-A' section.

The spatial distribution of apparent resistivity for the 3D model was calculated for the dipole-dipole array with the same parameters as for the 2D models. Inversion of the obtained data was performed in the Res3Dinvx64 software [18] using similar parameters as for the inversion of 2D data. Due to the different nature of the 3D inversion, it is not possible to use identical parameters that can be used in 2D inversion. The results of 3D inversion are presented in two ways in Figure 4. In the first case, from the interpreted resistivity block, the overburden layer and unpolluted aquifer were removed, thanks to which the interpreted pollution tongue which lay on the low resistivity substrate was exposed (Fig. 4a,b). The second way consisted in showing selected 2D sections being "cuts" made by the interpreted block (Fig. 4c,d,e).

### 3 Results and analysis

In the case of both 2D models (Fig. 2), the horizontal boundaries have been interpreted well. Interpreted resistivity values of individual layers are almost identical to those assumed. The sharp boundary for the M2 model has also been interpreted well. The only difference to the modelled situation is the appearance of an undervalued resistivity zone of the clay layer under the mentioned boundary. In the resultant section it looks like pollution tongue has penetrated

into the clay layer. The gradient boundary zone for the M1 model has been interpreted in a generalized way. From the right side it takes a vertical character, while from the left it shows the correct tilt. This is probably related to the subtle resistivity changes within the transitional zone assumed in the model. Such changes, due to the resolution of the DC-resistivity method, are not large enough to be interpreted. Nevertheless, the general shape and location of the discussed zone have been reflected satisfactorily.

Comparing the 3D modeled situation (Fig. 3) with the inversion results (Fig. 4), it can be concluded that its interpretation is very good. The shape of the pollution tongue is similar to the modelled one. Also, the interpreted resistivity values are almost identical comparing to modelled ones. Within the pollution cloud, the interpreted resistivity value is about 3 Ωm. In the case of clay layer, the interpreted values are generally the same as the assumed value of 10 Ωm.

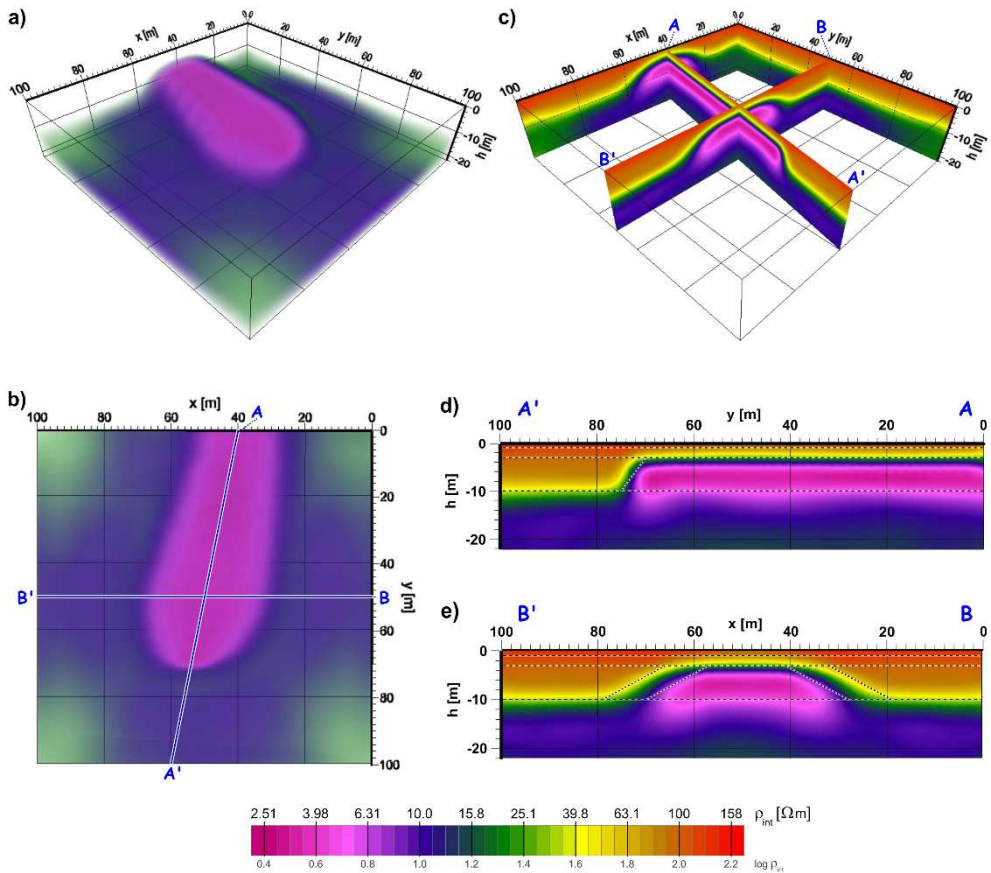


**Fig. 4.** Inversion results for the 3D pollution tongue model. Exposed substrate layer together with the tongue: a) general view; b) bird's eye view. 2D sections obtained from the 3D inversion results: c) general view; d) section A-A'; e) section B-B'.

In the A-A' section (Fig. 4d) the front of pollution tongue is not as sharp as for the result for a 2D M2 model (Fig. 2). Both situations, although they simulate a similar type of transitional zone between the clean and contaminated centre, may reflect it in different ways. It seems that better results were obtained for the inversion of 2D data. The difference is probably related to the fact that the 2D model assumes the constancy of the medium in the direction perpendicular to the section plane, while in the case of the 3D model it is more

complicated. In the direction corresponding to the x-axis there are changes in model structures and the 3D inversion algorithm takes them into account. However, in both situations, the phenomenon of the pollution tongue penetrating the low resistivity clay layer is visible. It has a much stronger character for 2D data (Fig. 2 - M2). It follows that the 3D inversion more accurately reflects the assumed model.

The case of the B-B' section (Fig. 4e) raises the problem of interpreting the gradient zone between the contaminated and clean centers. As can be seen it is interpreted very well. Moreover, the phenomenon of pollution cloud penetrating the bottom layer is observed, similarly as in 2D M1 model (Fig. 2). Due to the interpretation of the transitional zone fragment mentioned for the 2D case, it can be concluded that the situation has been better represented for 3D inversion results, where we do not deal with such a phenomenon.

## 4 Conclusions

On the basis of the analysis of the presented geoelectrical models and the obtained inversion results, the following conclusions were formulated:

- The 2D and 3D numerical modeling shows that the ERT method in both (2D, 3D) variants is suitable for solving the problem of groundwater contamination with soluble chemical substances;
- The ERT method appears to be promising in terms of the ability to detect and assess the nature of the transitional zone between clean and contaminated waters. However, for a real geological structure, especially within Quaternary formations, this task may be difficult and ambiguous. It seems simpler to effectively use electrical resistivity tomography method to study the behaviour of the pollution tongue in the aquifer in a monitoring system, especially using the 2D ERT;
- 3D ERT, due to the technical requirements (e.g. the use of a large number of electrodes to cover the research area), can be difficult to apply in the real field situation. Nevertheless, it may be very useful in the form of modeling for directing 1D and 2D DC-resistivity measurements;
- Analysis of 3D models can help to reduce to a certain extent the equivalence associated with the impact of spatial center structure on the 2D ERT measurements results.

The research presented in this paper was supported by the Dean's Grant no. 15.11.140.221.

## References

1. T. Dahlin, *First Break* **14**, 1137 (1996) doi: 10.3997/1365-2397.1996014
2. C. Bernstone, T. Dahlin, T. Ohlsson, H. Hogland, *Environ. Geol.* **39**, 360–371 (2000) doi: 10.1007/s002540050015
3. L.N. Meads, L.R. Bentley, C.A. Mendoza, *Can. Geotech. J.* **40**, 551–558 (2003) doi: 10.1139/t03-017
4. S. Lasocki, J. Antoniuk, W.J. Mościcki, *Environmental Protection Problems in the Vicinity of the Zelazny Most Flotation Wastes Depository in Poland*, *J. Environ. Sci. Heal. A* **38**, 1435–1443 (2003)
5. J.E. Chambers, O. Kuras, P.I. Meldrum, R.D. Ogilvy, J. Hollands, *Geophysics* **71**, B231-B239 (2006) doi: 10.1190/1.2360184

6. P. Martinez-Pagan, A.F. Cano, E. Aracil, J.M. Arocena, *Electrical Resistivity Imaging Revealed the Spatial Properties of Mine Tailing Ponds in the Sierra Minera of Southeast Spain*, J. Environ. Eng. Geoph. **14**, 63–76 (2009)
7. R. Clement, M. Descloitres, T. Gunther, L. Oxarango, C. Morra, J.P. Laurent, J.P. Gourc, Waste Manage. **30**, 452–464 (2010) doi: 10.1016/j.wasman.2009.10.002
8. G. Bania, M. Ćwiklik, 76th EAGE Conference and Exhibition 2014, Amsterdam, Netherlands, EAGE Publications BVNetherlands (2014) doi: 10.3997/2214-4609.20140966
9. G. Bania, M. Ćwiklik, 77th EAGE Conference and Exhibition 2015, Madrid, Spain, EAGE Publications BVNetherlands (2015) doi: 10.3997/2214-4609.201412539
10. W.J. Mościcki, G. Bania, M. Ćwiklik, M. Florek-Odrzyl, *Budowa utworów przypowierzchniowych na terenie zespołu dworsko-parkowego w Branicach koło Krakowa – wyniki badań elektrooporowych (The subsurface structure of manor-park complex in Branice near Krakow - the geoelectrical research)*, Nawarstwienia historyczne miast Europy Środkowej, Wydawnictwa AGH, Krakow, 407–423 (2016) (in Polish)
11. J. Antoniuk, W.J. Mościcki, *Investigation of polluted underground water with electrical and electromagnetic methods. Case of the „Zelazny Most” settling reservoir*, 2nd meeting “Environmental & Engineering Geophysics”, Nantes, France, 339–342 (1996)
12. J.J. Fried, *Groundwater pollution. Theory, methodology, modelling, and practical rules*, Elsevier Scientific Pub. Co, Amsterdam, New York. Developments in water science 4 (1975)
13. N.B. Dortman, *Petrophysics*, Reference Book, Book one, Rocks and mineral deposits. Nedra, Moscow (1992)
14. M.H. Loke, *Rapid 2D resistivity and I.P. forward modeling using the finite-difference and finite-element methods*, Geotomo Software, Manual (2016)
15. G. Bania, M. Ćwiklik, *Geology, Geophysics & Environment* **39**, 331 (2013) doi: 10.7494/geol.2013.39.4.331
16. M.H. Loke, *Rapid 2D Resistivity & IP Inversion using least-squares method*, Geotomo Software, Manual (2010)
17. M.H. Loke, *3-D resistivity & IP forward modeling using the finite-difference and finite-element methods*, Geotomo Software, Manual (2014)
18. M.H. Loke, *Rapid 3-D Resistivity & IP inversion using the least-squares method*, Geotomo Software, Manual (2016)